The need for clinical quantification of combined PET/MRI data in pediatric epilepsy

Otto Muzik [a,b,*], Darshan Pai [c], Csaba Juhasz [a], Jing Hua [c]

[a] Department of Pediatrics, Wayne State University School of Medicine, Detroit, MI, USA
[b] Department of Radiology, Wayne State University School of Medicine, Detroit, MI, USA
[c] Department of Computer Science, Wayne State University School of Medicine, Detroit, MI, USA

ARTICLE INFO

ABSTRACT

In the past, multimodality integrative analysis of image data has been used to obtain a better understanding of underlying mechanisms of seizure generation and propagation in children with extratemporal lobe epilepsy. However, despite important advances in the combined analysis of PET, MRI, DTI and EEG data, successful surgical outcome is only achieved in about 2/3 of patients undergoing resective surgery. The advent of simultaneous PET/MR data acquisition promises an important advance in neuroimaging through clinical quantification, which will finally translate the strength of PET (which is the ability to absolutely quantify physiological parameters such as metabolic rates and receptor densities) into clinical work. Taking advantage of recently developed integrated PET/MR devices, absolute physiological values will be available in clinical routine, replacing currently used visual assessment of relative tissue tracer uptake. This will allow assessment of global increases/decreases of brain function during critical phases of development and is likely to have a significant impact on patient management in pediatric epilepsy.

1. The importance of simultaneous PET/MR data acquisition in neuroimaging

In the last decade PET/CT showed the added value of multimodality integration for both research and clinical assessment of cancer, and this form of imaging became within a few years the state-of-art in diagnostic oncology. In fact, since 2000, the world market share of PET/CT scanners increased from less than 5% to more than 95%, thereby completely replacing dedicated PET scanners. The added value provided by combined PET and CT imaging has improved both the localization and staging of tumors in addition to significantly increasing patient throughput. Although current PET/CT scanners acquire the image data sequentially (initial helical CT scan is followed by multiple bed position PET imaging), this is usually of little consequence for tumor assessment, as only the overall PET tracer distribution, established following an extended uptake period, is of clinical interest.

In contrast, the situation is fundamentally different in neuroimaging, where MR data is highly superior to CT not only due to the excellent gray/white matter contrast but also due to the possibility of obtaining high-resolution information with respect to fiber tracts and fast changing blood flow patterns. Thus there are fundamental advantages to the simultaneous acquisition of PET and MR data for neuroimaging, that reach far beyond simple coregistration of the two image volumes (which can be relatively easily performed for rigid objects such as the brain within a skull). The true advantage of simultaneous PET/MR acquisition lies in the ability to offset one modality's limitations (e.g., limited resolution in PET or the limited functional information inherent in MR) through data derived simultaneously from the complementing modality – thus providing not just an additive, but multiplicative effect. This exchange of complementary information can be taken into account already at a very basic hardware level, so that many issues, presently only poorly accounted for during image post-processing (motion artifacts, partial volume distortions), become irrelevant.

The simultaneous acquisition of complementary information has the potential to significantly advance the field of neuroimaging through **clinical quantification**, which will deliver quantitative values of physiological parameters into the clinical arena. As a result, absolute values representing metabolic rates, receptor densities or binding potentials will be available to the physician directly in the clinical routine and will play an increasingly important role in clinical management decisions. The prospect of clinical quantification represents an important advance in neuroimaging, as it finally translates the strength of PET (i.e. absolute quantification of physiological parameters) into the

* Correspondence to: PET Center, Children's Hospital of Michigan, 3901 Beaubien Blvd, Detroit, MI 48201, USA. Tel.: +1 313 993 2616.
E-mail address: otto@pet.wayne.edu (O. Muzik).

clinical assessment of patients. Consequently, simultaneous PET/MR imaging has the potential to change the clinical landscape of neuroimaging in a similar way as PET/CT did a decade ago for oncology.

However, in order to achieve this ultimate goal, several software challenges need to be addressed. The most crucial issues that need to be solved is the fully automated determination of an image-derived arterial input function as well as the on-the-fly motion correction of PET line of responses (LORs) in order to correct for patient motion. In addition, a cohesive computational framework needs to be developed that facilitates the understanding of qualitatively different data sets in a larger context. Important features of such an integrative computational framework is an advanced 3D visualization of processed image volumes as well as quantitative description of data properties, so that relationships in anatomical and functional domains between complementing modalities can be expressed in a closed mathematical form. By taking advantage of advanced data integration schemes, quantitative results can be subsequently combined into data structures that provide a consistent framework for the application of advanced data mining techniques. As an example, such multimodality database structures hold promise of providing new insights into the formation, identification and maturation of epileptic foci and might lead to new approaches in epilepsy surgery that have the potential to improve clinical management of patients suffering from intractable epilepsy.

2. PET/MR application in pediatric epilepsy

Specifically in the context of pediatric epilepsy patient management, the relevance of simultaneous PET and MR acquisition is extraordinary. At present, all pediatric epilepsy patients undergo MR and PET imaging on two separate occasions, doubling the time/frequency of sedation and on-scanner time. The simultaneous acquisition of PET and MR will allow a more efficient use of both patient time and staff resources, and will significantly improve the logistics of patient scheduling and enrollment into research studies. More importantly, clinical quantification will allow assessment of absolute values for physiological parameters, removing a significant limitation of currently used tracer normalization schemes (as discussed below). Finally, the combination of various PET tracers with diffusion tensor imaging (DTI, allowing assessment of fiber tract connectivity), MR volumetry (morphology) and BOLD MR (blood flow) acquired simultaneously is likely to bring new insights into the study of seizure generation and propagation. As an example, PET/MR imaging could provide the unique opportunity to measure simultaneously both pre-synaptic (short echo proton MR spectroscopy) and postsynaptic (C11-flumazenil PET) aspects of GABA neurotransmission during interictal periods. Moreover, the combination of PET with high resolution MR spectroscopy (MRS) could provide a significant advantage, as a preliminary PET image (reconstructed using data from the initial part of the PET study) could be used to guide the definition of several large MRS regions. This approach would be more efficient than is a whole brain coverage of MRS, especially in the case of substances such as GABA or glutamate that require a prohibitively long MRS scan time to yield clinically acceptable sensitivity.

In the past, several groups have successfully used combined data from independently acquired PET, MR and EEG in the presurgical evaluation of epileptic children [1,2]. This multimodality approach resulted in a significant improvement in surgical outcome, although still about one in three patients fail to become seizure free following resective surgery. It appears that further improvements in the localization of epileptogenic brain tissue can

only be derived from novel data acquisition schemes that facilitate the development of a unifying computational framework that gracefully integrates qualitatively diverse data sets within a common reference frame. As a result, meta-analyses of data patterns that are distributed over several modalities can be undertaken and are likely to provide "added value" when assessing the state of the epileptic brain. Obviously, such analyses require in addition to a formal mathematical structure also well-developed visual interface tools that allow researchers to grasp the relationship between data patterns in an intuitive way and provide clinicians with important clues regarding the pathological state of brain tissue under study.

2.1. The problem of brain surface parcelation

The first step in the direction of a successful integrative computational framework for brain analysis is to achieve a mathematically consistent parcelation of the brain surface in native space. The result of such a parcelation is the creation of homotopic cortical areas across patients, which is subsequently used to relate local cortical patient features to a normative value (which is derived from homotopic cortical areas in an age-matched group). Unfortunately, a consistent parcelation of anatomical brain surface structures from 3D image data and their compact geometrical representation in a rigorous computational framework proved extremely challenging. The reason for this is that boundaries and extent of gyri are imprecise and major sulci show frequently variable branching patterns or may be absent, even in the normal population. Owing to the limitations of template space approaches for the study of patient data in a clinical setting, we have developed a cortical parcelation scheme that takes advantage of user-defined cortical landmarks that are conformally mapped from native space into a spherical domain [3,4]. The landmarks are then aligned in the spherical domain and a fractal (regular) parcelation of the sphere is then applied. This yields finite surface elements that have identical spatial relationship to cortical landmarks across different subjects (Fig. 1). The final step consists then in the inverse mapping ("unwarping") of landmarks back into native space, positioning each finite surface element into native space in such a way that their spatial relationship to the landmarks is unchanged. As the spatial relationship between cortical landmarks and finite elements is identical in each subject, the resulting finite surface elements are homotopic across individual subjects (i.e. they conform spatially) and can be used as basic elements of analysis within an integrative framework.

2.2. Integration of multimodality data in the presurgical evaluation of epilepsy patients

Following parcelation of the cortex, the PET tracer concentration in finite cortical elements is sampled using inverse gradient fusion (depth of 5–10 mm), and the extent and severity of PET abnormalities can be then objectively assessed in relationship to electrophysiological information. Application of this method to pediatric epilepsy cases suggests that cortical areas surrounding FDG PET defined hypometabolic regions (2 cm border zone area, see Fig. 2) detect a similar proportion of onset electrodes as hypometabolic areas do (46% vs. 41%) [5].

Thus the predictive value of FDG PET is close to 90% if border zone areas are considered for seizure onset localization. These findings strongly support the notion that seizure onset areas often extend beyond the hypometabolic cortex to encompass adjacent normo-metabolic areas, while a large portion of the hypometabolic cortex is not involved in seizure onset or early seizure propagation. As a result, clinical utility of FDG PET in guiding
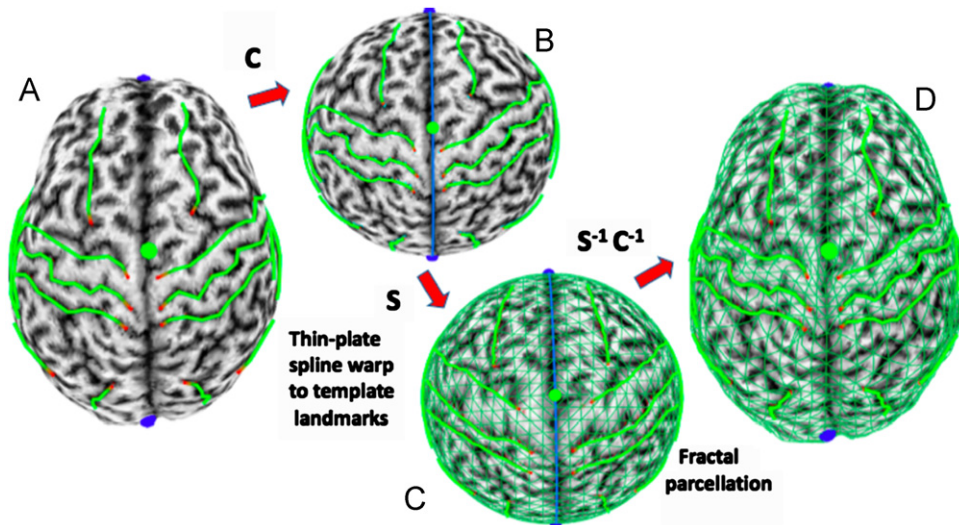
Fig. 1. Sequence of steps to perform a landmark-constrained conformal mapping of the cortical surface. (A) Manually defined landmarks. (B) Conformal mapping into spherical domain. (C) Thin-plate warp of landmarks to template and fractal parcelation to create finite cortical elements. (D) Inverse mapping of finite cortical elements into native space. As the spatial relationship between cortical landmarks and finite cortical elements is identical, the resulting cortical finite elements are homotopic across individual subjects, i.e. conform spatially.
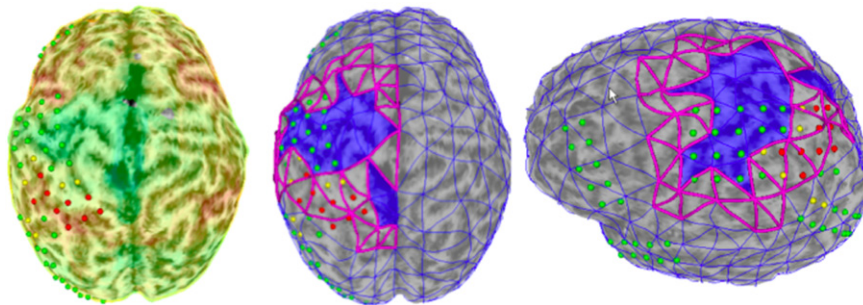

Fig. 2. Integration of FDG PET, MR and EEG data to assess the spatial relationship between epileptogenic and hypometabolic cortex. EEG grid electrodes are color-coded as red (seizure onset), yellow (early seizure propagation) and green (normal). Location-specific asymmetry thresholds were applied to the FDG PET image (left), yielding objectively determine hypometabolic cortical areas (highlighted in blue, center and right). It is apparent that seizure onset electrodes (red) are preferentially located in the normometabolic borderzone (finite elements highlighted in purple) as opposed to the hypometabolic cortex. (For interpretation of the references to color in this figure legend, the reader is referred to the web version of this article.)

subdural electrode placement is greatly enhanced if grid coverage is extended to at least 2 cm beyond the FDG PET defined hypometabolic areas (Fig. 2).

2.3. Assessment of connectivity between the primary focus and remote areas

At present, the relevance of cortical hypometabolic areas observed by PET imaging that are located remotely to the primary seizure focus (and are shown to be electrophysiologically normal) is poorly understood. The fate of such remote functional abnormalities following resection of the primary epileptic focus remains uncertain. Cortical areas showing functional abnormalities on PET can either normalize following resection of the primary focus or may mature to become independent primary foci. Consequently, the goal of integrative image analysis in epilepsy is to predict whether a remote functional abnormality will likely become a future seizure onset area that needs to be resected, or whether this area will normalize and thus can be spared during surgery. With the advent of diffusion tensor imaging (DTI), it became possible to study connectivity among cortical brain areas in vivo. More importantly, quantitative assessment of connectivity between cortical areas appears to be an essential part in our understanding of the mechanisms underlying the origin and maturation of these secondary epileptic foci. In order to quantitatively assess the

connection strength between EEG-defined epileptogenic brain areas and other territories, we have adapted a Bayesian probabilistic method [6] for fiber tracking in order to find a connectivity threshold that would discriminate between brain areas that will mature to become an independent seizure focus or will normalize. To calculate the connectivity strength between a source and target region, the average probability p_i is calculated for each individual fiber path i of length N_i as

$$p_i = N_i \sqrt{\prod_{j=1}^{N_i} p_{ij}} \qquad (1)$$

where p_{ij} is the randomly sampled probability of voxel j ($j=1,..N_i$). Because only a subset of fibers originating from the seed region will terminate in the target region, all path probabilities p_i are subsequently normalized to the sampling space (total number of fiber paths $k=1,...,M$) as p_i':

$$p_i' = \frac{p_i}{\sum_{k=1}^{M} p_k} \qquad (2)$$

Finally the normalized probability score of connection between two regions A and B is obtained as P_{A-B}

$$P_{A-B} = \sum_{l=1}^{L} p_i' \qquad (3)$$

with the index l ($L < M$) representing all fiber paths connecting the two regions. As an example consider the two fiber paths shown in Fig. 3. The local probability density function (PDF) is determined at each step location based on the PDF of the neighboring 8 image voxels, weighted by the distance from the current position. Starting from a seed point, random samples are drawn from the PDF and fiber paths are created which terminate when the local fractional anisotropy (FA) decreases below a pre-selected value (usually 0.15). It has to be noted that this model assumes only one fiber direction in each voxel (single-fiber model) and any deviation from this model (such as fiber crossing/convergence) is translated into
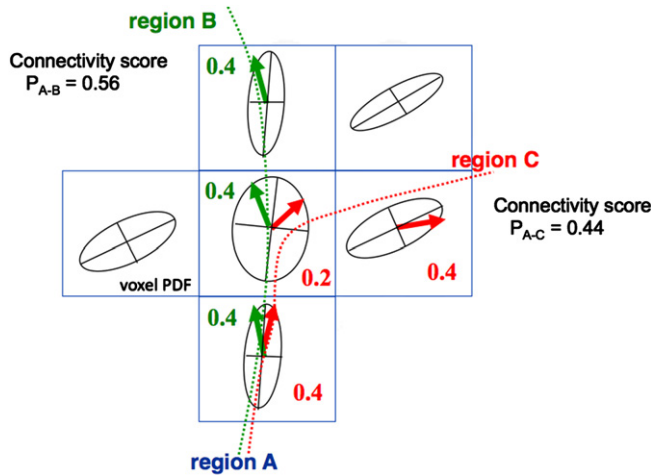

Fig. 3. Assessment of the connectivity strength between cortical regions using probabilistic fiber tracking. Starting from a seed region (region A), random samples are drawn from the calculated probability distribution function (PDF) in each image voxel. The figure shows two paths consistent with the data: a path that connects regions A and B (green) and a path that connects regions A and C (red). The higher average probability along path A–B as compared to path A–C is reflected in the higher connectivity score for P_{A-B}. (For interpretation of the references to color in this figure legend, the reader is referred to the web version of this article.)

uncertainty in the PDF. This uncertainty leads then locally to an increased probability of randomly sampled fibers to diverge into multiple directions, thus allowing a certain portion of fiber paths to cross low-anisotropy areas, hence realizing minor fiber tracks. Starting from region A, random samples are drawn from the calculated PDF in each image voxel, yielding ∼10,000 paths originating from the source region. The average probability p_i for each path is calculated (Eq. (1)) and subsequently normalized so that the total probability to reach any brain region equals to 1 (p_i', Eq. (2)).

The connectivity strength between two cortical regions (A–B or A–C) is then calculated as the sum of all path probabilities terminating in the particular target region (PA–B or PA–C, Eq. (3)). In the example above, the average probability along path A-B is $(0.4 \times 0.4 \times 0.4)^{1/3} = 0.4$ and is $(0.4 \times 0.2 \times 0.4)^{1/3} = 0.36$ along path A–C. The total probability for the two fibers is 0.72 ($=0.32+0.40$) and the connectivity strength to reach region B ($0.4/0.72=0.56$) is higher than to reach region C ($0.32/0.72=0.44$).

3. Results

We have applied multimodality data integration of MR, PET, EEG and DTI data in the past in order to maximize surgical success of pediatric epilepsy surgery. Until now, all modalities had to be acquired independently and integrated in a complex post-processing analysis, limiting both the feasibility and potential of this approach. As an example, Fig. 4 shows a representative example of our analysis in a patient with extratemporal lobe epilepsy. A 2D map of the patient's left hemisphere shows the proximity of seizure onset (red +) as well as electrophysiologically normal (green +) electrodes to abnormally decreased (blue and purple) and increased (yellow and red) FDG PET tracer concentrations (Fig. 4, panel A). Elements that are associated with seizure onset electrodes are depicted as a black-boarded area that was used as source region for probabilistic fiber tracking. The obtained normalized probability score values are rendered as small dots in the center of the finite elements and
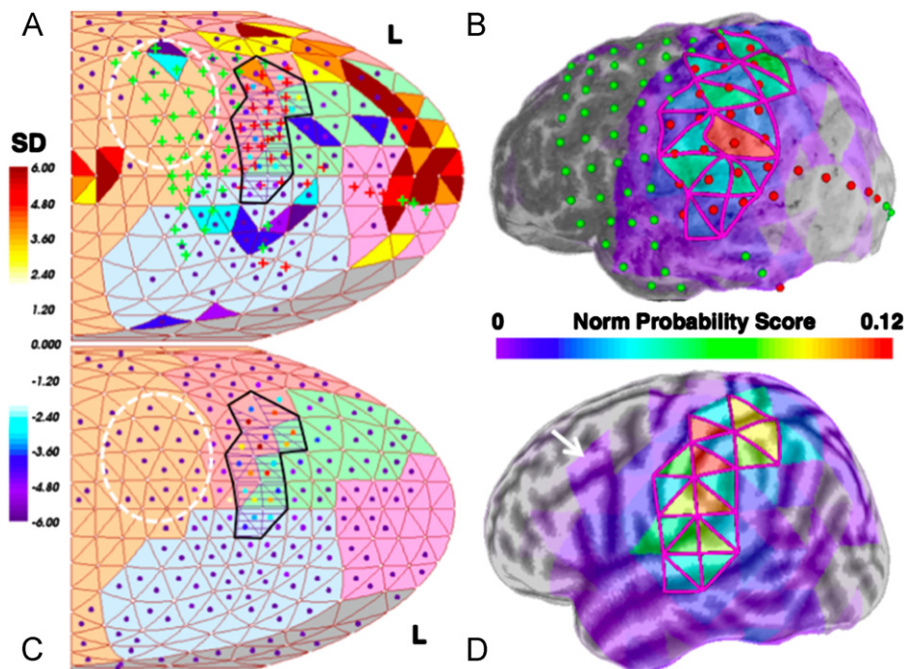

Fig. 4. Integrative analysis of EEG, PET and DTI data in 2D representation allows simplified assessment of the spatial relationship between these three modalities during surgical conference. (For interpretation of the references to color in this figure legend, the reader is referred to the web version of this article.)

color-coded from 0 (no dot) to a maximum value of 0.12 (red). The corresponding surface view (Fig. 4, panel B) shows all source elements used for probabilistic fiber tracking as well as the normalized probability score rendered onto the cortical surface together with the location of seizure onset (red) and electrophysiologically normal (green) electrodes. Finally, panel C shows a 2D representation of the average distribution pattern representing the normalized probability score values derived from a pediatric (age-matched) control group. Statistical analysis revealed a significantly lower probability score to the frontal lobe in the patient (white broken circle) as compared to the control group. The corresponding surface view (Fig. 4, panel D) shows increased number of finite elements with non-zero probability score in the frontal lobe of the control group (white arrow). Despite demonstrating a significantly decreased connectivity score between areas of the primary seizure focus (as defined by the gold standard of intracranial electrocorticography) and remote PET abnormalities, definition of a threshold that would identify future secondary foci proved so far elusive.

4. The relevance of clinical quantification for pediatric epilepsy

A possible reason for the clinical problem of identifying secondary epileptic foci prior to their maturation is likely related to the currently applied method for objective definition of cortical PET abnormalities. Because arterial blood sampling is impossible in the clinical routine, the obtained data cannot be converted into physiological values (e.g. metabolic rate of glucose in umol/100 g/min) and as a result only the tracer concentration is available. As a consequence, in order to compare the patient's tracer concentration against normative values, the tracer concentration in each voxel is normalized to the patient's average brain tracer concentration. These approaches result (for each finite cortical element) in abnormal increase (shown in yellow–orange–red in Fig. 4) or abnormal decrease (shown in light blue–dark blue–purple in Fig. 4) of PET tracer concentration. Although this normalization approach is by necessity frequently used in clinical routine, it is flawed due to the patient's (most likely abnormal) PET tracer

uptake pattern. As the tracer concentration in an epileptic brain can be both locally increased or decreased, normalization to the average brain tracer concentration (even when performed to the contralateral hemisphere) is problematic and likely to affect the definition of PET abnormalities. Moreover, in contrast to oncology where the absolute glucose metabolic rate of the tumor is of lesser importance, glucose metabolic rate of the brain changes drastically during development. Brain glucose metabolism follows a steep rise from birth to about 6 years of age, remains at a plateau until 10–12 years of age and then declines exponentially to adult values, which are about 50% that of the peak values. Thus in the absence of absolute values it is not clear whether local increases of FDG tracer concentration represent true hypermetabolism or possibly abnormal decreases in glucose metabolism of adjacent brain areas. Especially in the pediatric population the determination of absolute physiological values will be of great clinical interest and most likely will provide additional clues with respect to the maturation of secondary epileptic foci. Finally, the possibility to have individual patients' absolute values available might revolutionize the way statistical parametric mapping (SPM) analysis is performed, as it will be possible to model the main effect and not only pattern differences. This in return will allow assessment of global increases/decreases of brain metabolism during critical phases of development. As such, the advent of simultaneous PET/MR is likely to have a significant impact on patient management in pediatric epilepsy.

References

[1] E. Asano, C. Juhász, A. Shah, O. Muzik, D.C. Chugani, J. Shah, S. Sood, H.T. Chugani, Epilepsia 46 (7) (2005) 1086.
[2] K. Kagawa, D.C. Chugani, E. Asano, C. Juhász, O. Muzik, A. Shah, J. Shah, S. Sood, W.J. Kupsky, T.J. Mangner, P.K. Chakraborty, H.T. Chugani, Journal of Child Neurology 20 (5) (2005) 429.
[3] G. Zou, J. Hua, O. Muzik, Medical Image Computing and Computer-Assisted Intervention 10 (2007) 367.
[4] O. Muzik, D.C. Chugani, G. Zou, J. Hua, Y. Lu, S. Lu, E. Asano, H.T. Chugani, International Journal of Biomedical Imaging (2007) 13963.
[5] B. Alkonyi, C. Juhasz, O. Muzik, E. Asano, A. Saporta, A. Shah, H.T. Chugani, Epilepsy Research 87 (2009) 77.
[6] O. Friman, G. Farnebäck, C.F.A Westin, IEEE Transactions on Medical Imaging 25 (8) (2006) 965.